Applied Numerical Modeling in Geomechanics – 2020 – Billaux, Hazzard, Nelson & Schöpfer (eds.) Paper: 01-07

PFC2D modelling of sinkhole cluster in karstic depressions

Djamil Al-Halbouni[1,2], Sacha Emam[3], Eoghan P. Holoan[4], Abbas Taheri[5], Martin P.J. Schöpfer[6] & Torsten Dahm[1,2]

[1] *Helmholtz Centre - German Research Centre for Geosciences (GFZ), Physics of Earthquakes and Volcanoes, Telegrafenberg, Potsdam 14473, Germany*

[2] *University of Potsdam, Institute of Geosciences, P.O. Box 601553, Potsdam-Golm 14415, Germany*

[3] *Itasca Consultants S.A.S., Écully, France*

[4] *UCD School of Earth Sciences, University College Dublin, Belfield, Dublin 4, Ireland*

[5] *School of Civil, Environmental and Mining Engineering, University of Adelaide, Adelaide, South Australia 5005, Australia*

[6] *Department for Geodynamics and Sedimentology, University of Vienna, Athanstrasse 14, A-1090, Vienna, Austria*

1 INTRODUCTION

Sinkholes are a common natural hazard in karst areas worldwide. In such areas, where geologic materials are rich in evaporite or carbonate minerals, voids can form in the underground by chemical and physical removal of subsurface material (Waltham & Fookes 2005). Collapse of the overburden of such voids is a mechanism to generate sinkholes. At the Dead Sea, the fall of the lake level since 1970 has been linked to the appearance of over 7,100 sinkholes in the last 35 years, which has been related to void generation by dissolution and physical erosion of subsurface evaporite deposits (halides, carbonates, and sulphates, Abelson et al. 2017, Al-Halbouni et al. 2017). This study focusses on the Ghor Al-Haditha sinkhole area at the SE border of the Dead Sea, where over 1000 sinkholes have been registered (Watson et al. 2019, Fig. 1).

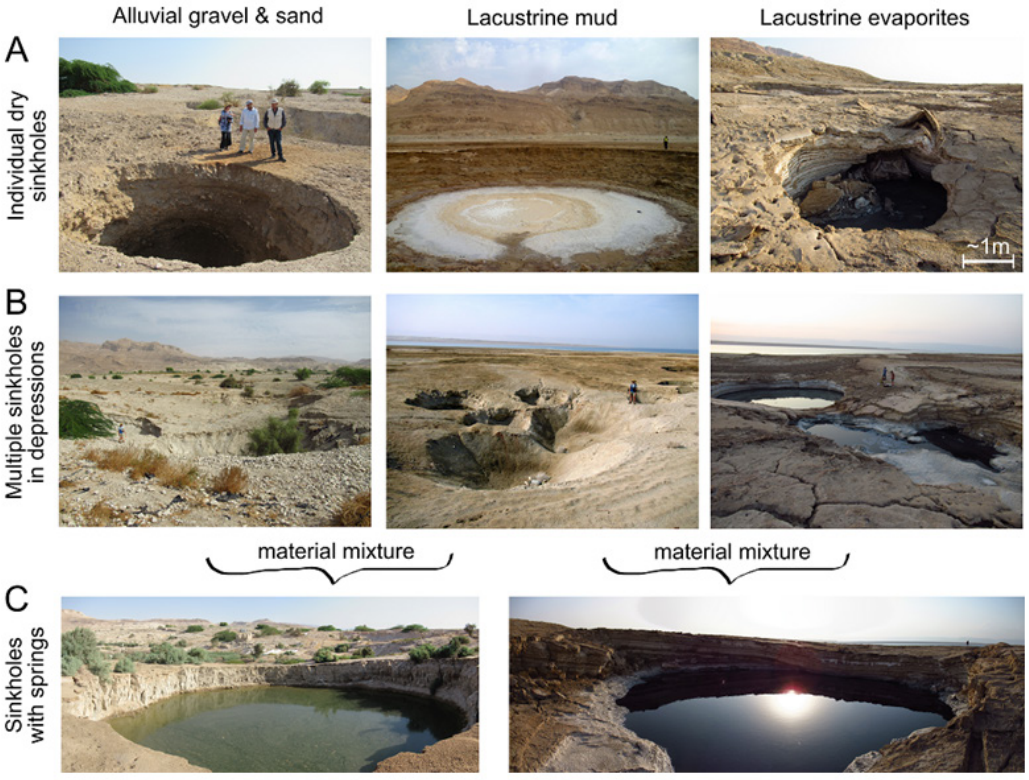

Figure 1. Different forms of sinkholes at Ghor Al-Haditha, Jordan. (A) examples of individual sinkholes in the three typical cover materials (alluvium, mud and evaporites). (B) multiple sinkholes and larger-scale depression in the same materials. (C) sinkholes in material mixtures and associated with active springs. Note persons/infrastructure for scale.

Sinkholes at Ghor Al-Haditha, and at the Dead Sea generally, fall between two main morphological endmembers: (1) flat and wide sinkholes in mud-flats comprising the former lake bed; (2) narrow and deep sinkholes in the alluvium or thick evaporite cover (Fig. 1A). While this distinction generally holds for individual sinkhole endmembers, mixtures of both types and both materials occur. Also, coalesced/nested multiple sinkholes developed over time in this area (Fig. 1B & 1C). This development is related to a maturation of the karst system and occurs with the formation of larger-scale uvala-like depressions (Watson et al. 2019). In this paper we summarize the usage of the Distinct Element Method (DEM), as implemented in *PFC2D* version 5.0 (Potyondy & Cundall 2004, Itasca 2014), to simulate sinkhole and depression formation (Al-Halbouni et al. 2018, 2019). We relate morphology and collapse style to material strength and material combination, and we provide an overview of the implemented parameter tracking possibilities.

2 DESIGN AND ANALYSIS

In *PFC2D* version 5.0, disk-shaped particles interact through binary contacts, and the Newton/Euler laws of motion are used to update their kinematics. The resulting differential equations are solved via a finite-difference, explicit, time-stepping algorithm (Itasca 2014). In this study, a particle assembly is first generated via a randomized packing scheme and gravitational settling (Al-Halbouni et al. 2018), using a linear elastic force-displacement law. After this stage, particles are bonded with their neighbors, using the parallel-bond model (PBM, Potyondy & Cundall 2004, Potyondy 2014), which sets a second pair of elastic springs that incorporate moments and can fail either in shear or tension. Bond failure leads to fracturing and strain localization within the bonded particle assembly and allows for emergence of a complex elasto-plastic rheology (Al-Halbouni et al. 2018, Holohan et al. 2011, Potyondy & Cundall 2004, Schöpfer et al. 2009).

For simulation of sinkhole formation, growth of cavity sets within the assembly was simulated by particle removal (Fig. 2). A linear void space growth function related initial void space area with the removed area at further intervals. This acted as a proxy for real void growth by subsurface physio-chemical processes (i.e. subrosion).Optimal model dimensions of H × W = 400 × 400 m with particle radii uniformly distributed between 0.2 m and 0.4 m were determined via a benchmarking procedure for surface displacements (Al-Halbouni et al. 2018). The cavity array could be set to an arbitrary depth and to arbitrary growth functions to mimic the distribution of focused or deepening mechanical erosion (cf. Al-Halbouni et al. 2019).

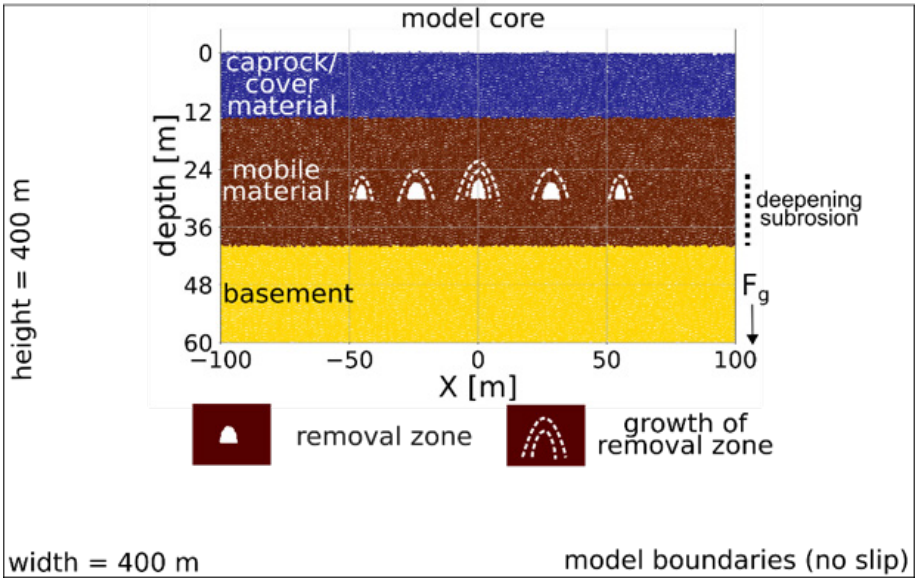

Figure 2. Generic setup for multiple and single cavity modelling with DEM. Shown is the core of the model with material removal zones in a layered system. Modified after Al-Halbouni et al. 2018, 2019.

Combinations of three different materials typical for the case-study area of the Dead Sea were tested: low-strength marly sediments (mud), middle strength sandy-gravel sediments (alluvium) and high-strength lacustrine evaporite deposits (salt). The material micro-properties and corresponding macro-properties, the latter obtained through simulated compression and tension tests, are listed in Table 1.

Table 1. Micro- and Macro-properties from simulated rock tests and a Mohr-Coulomb failure criterion.

Property/ Material	Symbol [unit]	Mud	Alluvium	Salt
Young's modulus	E [MPa]	100	200	1000
Parallel bond tensile strength	Pb_ten [MPa]	0.1	0.5	1.0
Parallel bond cohesion	Pb_coh [MPa]	0.5	0.02	1.0
Parallel bond friction angle	ϕ [°]	2.4	34	54
Density	ρ [kg/m3]	2715	2750	2500
Porosity	n	0.2	0.2	0.2
Bulk modulus	E_{bulk} [MPa]	84	174	1106
Bulk Poisson ratio	ν	0.2	0.31	0.3
Bulk unconfined compressive strength	UCS [MPa]	0.25	0.5	1.23
Bulk tensile strength	T [MPa]	0.2	0.24	0.43
Bulk friction angle	ϕ_{bulk} [°]	6	22	28.8
Bulk density	ρ_{bulk} [kg/m³]	2145	2200	2075

Overlapping measurement circles were used to determine porosity, displacement and stresses in the models. The algorithms from Hazzard (2014) are implemented for crack tracking and acoustic emissions monitoring. Seismicity and seismic moment can be derived, as seen in the composite plot of Figure 3 for a typical single sinkhole collapse, and seismic velocities can be computed (Al-Halbouni et al. 2019).

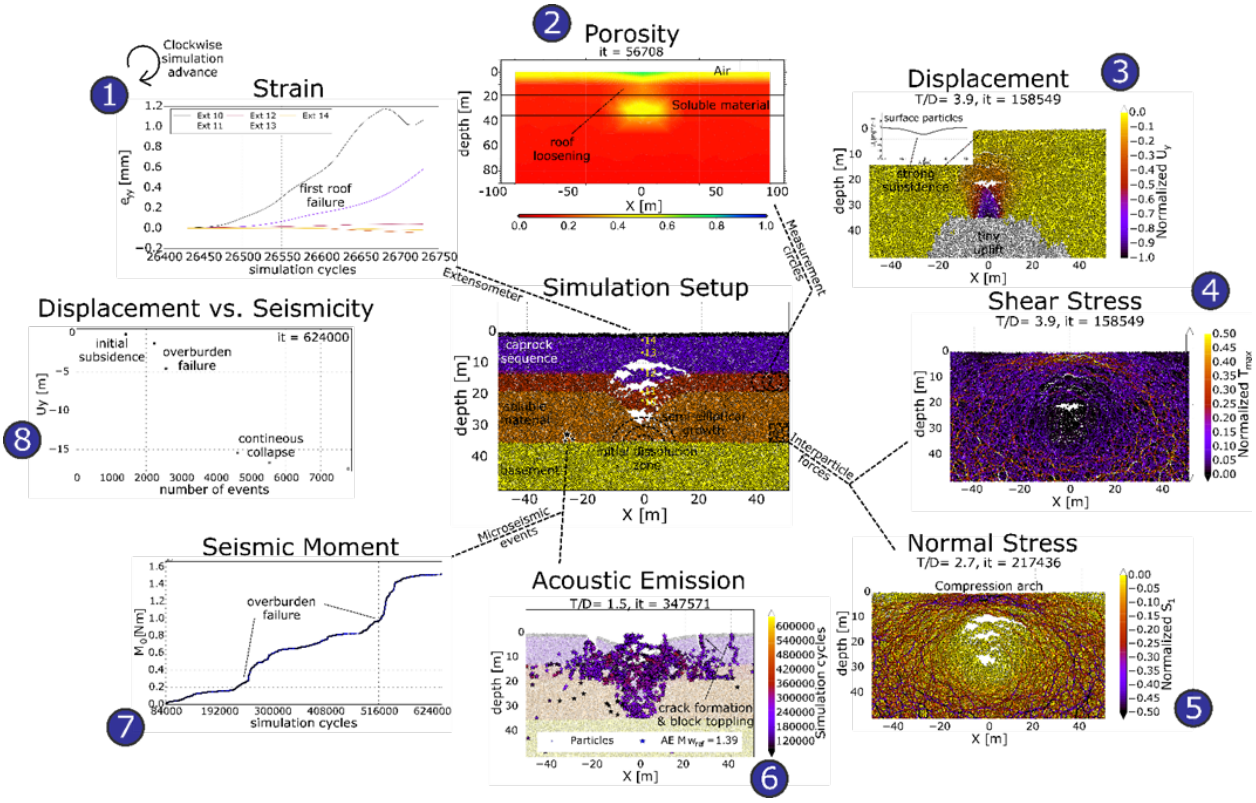

Figure 3. Schematic implementation of composite tracking of geophysical and geodetic signatures before, during and after collapse of a single sinkhole. The simulation time increases in clockwise direction. T/D means the cover thickness to diameter ratio, 'it' is the iteration number.

3 RESULTS AND DISCUSSION

Figure 4 shows a summary of results for different model setups. The individual sinkholes show clear morphological differences depending on the cover or host-rock material (Fig. 4A). Weak cover material like mud favors flat and wide sinkhole formation. Strong cover material like alluvium or salt favors deep and narrow sinkhole formation, commonly with overhanging sides. The multiple sinkholes lying within deeper depressions (Fig. 4B) were achieved with a deepening differential material removal technique. The collapse style is dependent not only on the material strength of the cover but also on that of the cavity-hosting material. Strong materials like salt favor brittle behavior and block-wise subsidence as well as coalescence of holes, while weak materials like mud favor depression widening and sagging structures.

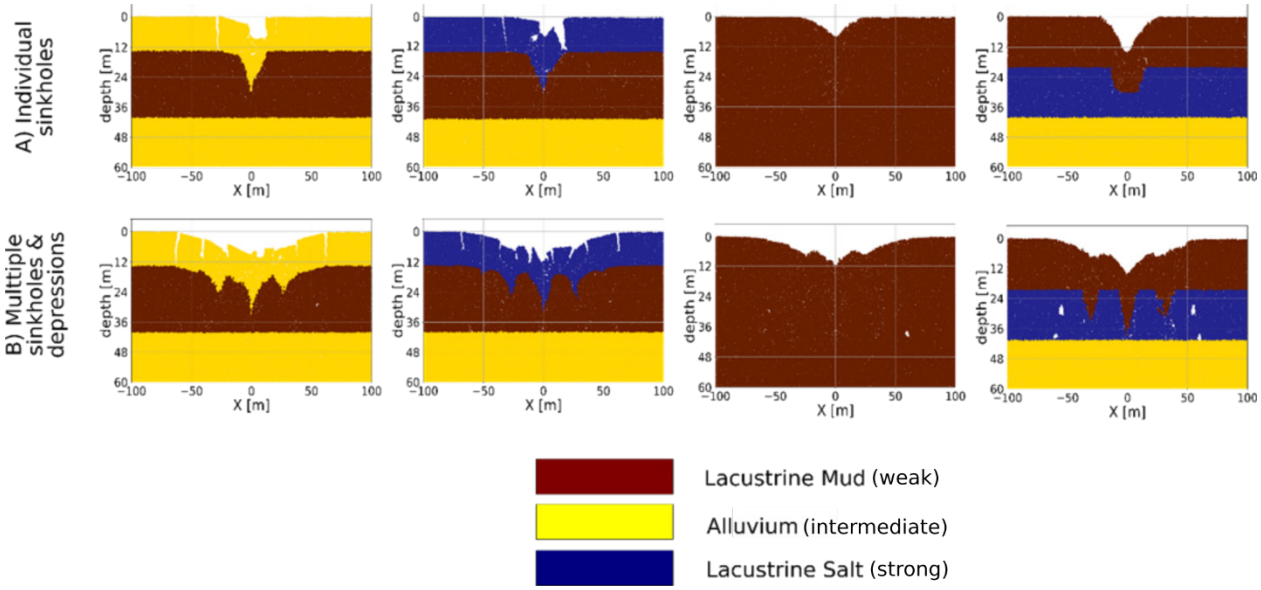

Figure 4. Endmembers for sinkholes and large-scale depressions. A) Individual sinkholes and B) multiple sinkholes within depressions. Layer colors represent the materials of varying mechanical properties (especially strength).

4 CONCLUSIONS

We successfully used *PFC2D* version 5.0 to make physically realistic simulations of the formation of sinkholes and large-scale karstic depressions. A flexible cavity growth procedure has been implemented to simulate failure processes in different materials commonly encountered at the Dead Sea sinkhole area. Resulting morphologies are in good agreement with field observations and reflect the dependency on classical rock strength parameters. Furthermore, a geodetic and geophysical parameter tracking procedure has been implemented which enables comparison of simulation results with field data. Thus, the developed simulation and tracking approach allows application for early warning of collapse processes.

ACKNOWLEDGEMENTS

The first author acknowledges the financial support by the Helmholtz DESERVE Virtual Institute and the Federal Ministry of Education and Research of Germany in the framework of SIMULTAN (grant 03G0843). Particular thanks go to Itasca for providing the license of *PFC2D* version 5.0 through the Itasca Educational Partnership.

REFERENCES

Abelson, M., Yechieli, Y., Baer, G., Lapid, G., Behar, N., Calvo, R. & Rosensaft, M. 2017. Natural versus human control on subsurface salt dissolution and development of thousands of sinkholes along the Dead Sea coast, *J. Geophys. Res. Earth Surf.*, 122(6), 1262–1277, doi:10.1002/2017JF004219.

Al-Halbouni, D., Holohan, E. P., Saberi, L., Alrshdan, H., Sawarieh, A., Closson, D., Walter, T. R. & Dahm, T. 2017. Sinkholes, subsidence and subrosion on the eastern shore of the Dead Sea as revealed by a close-range photogrammetric survey, *Geomorphology*, 285, 305–324, doi:10.1016/j.geomorph.2017.02.006.

Al-Halbouni, D., Holohan, E.P., Taheri, A., Schöpfer, M.P.J., Emam, S. & Dahm, T. 2018. Geomechanical modelling of sinkhole development using Distinct Elements : Model verification for a single void space and application to the Dead Sea area, *Solid Earth*, 9, 1341–1373, doi:10.5194/se-2018-62.

Al-Halbouni, D., Holohan, E.P., Taheri, A., Watson, R., Polom, U., Schöpfer, M.P.J., Emam, S. & Dahm, T. 2019. Distinct element geomechanical modelling of the formation of sinkhole clusters within large-scale karstic depressions, *Solid Earth*, *10*(4), 1219–1241, doi:10.5194/se-10-1219-2019.

Hazzard, J.F. 2014. Acoustic Emission Calculation in PFC5.0, Minneapolis, Minnesota, USA.

Holohan, E.P., Schöpfer, M.P.J. & Walsh, J.J. 2011. Mechanical and geometric controls on the structural evolution of pit crater and caldera subsidence*, J. Geophys. Res*., 116(B07202), doi:10.1029/2010JB008032.

Itasca Consulting Group, Inc. 2014. *PFC2D – Particle Flow Code in 2 Dimensions, Ver. 5.0 User's Manual.* Minneapolis: Itasca.

Potyondy, D.O. 2014. The bonded-particle model as a tool for rock mechanics research and application: current trends and future directions, *Geosystem Eng*., 17(6), 342–369.

Potyondy, D.O. & Cundall, P.A. 2004. A bonded-particle model for rock, *Int. J. Rock Mech. Min. Sci.,* 41(8), 1329–1364, doi:10.1016/j.ijrmms.2004.09.011.

Schöpfer, M.P.J., Abe, S., Childs, C. & Walsh, J.J. 2009. The impact of porosity and crack density on the elasticity, strength and friction of cohesive granular materials: Insights from DEM modelling, *Int. J. Rock Mech. Min. Sci.,* 46(2), 250–261, doi:10.1016/j.ijrmms.2008.03.009.

Waltham, A.C. & Fookes, P.G. 2005. Engineering classification of karst ground conditions, *Q. J. Eng. Geol. Hydrogeol*., 3(1), 1–20, doi:10.1144/1470-9236/2002-33.

Watson, R.A., Holohan, E.P., Al-Halbouni, D., Saberi, L., Sawarieh, A., Closson, D., Alrshdan, H., Abou Karaki, N., Walter, T.R. & Dahm, T. 2019. Sinkholes and uvalas in evaporite karst: spatio-temporal development with links to base-level fall on the eastern shore of the Dead Sea, *Solid Earth*, *10*(4), 1451–1468, doi:10.5194/se-10-1451-2019.

.